International Journal of Applied Engineering Research ISSN 0973-4562 Volume 10, Number 17 (2015) pp 37887-37893

An Improved Method for Segmentation of Abnormal Tissues in MRI Brain Images using Modified Entropy and Fuzzy C-Means Clustering Algorithm

Smitha J C
Research Scholar, Department of Computer Science, Noorul Islam Centre for Higher Education, Kumaracoil, Tamil Nadu
smithajc@gmail.com

Dr S Suresh Babu
Principal, Sree Buddha College of Engineering, Alapuzha, Kerala drssb@gmail.com

Abstract
The aim of this work is to present an automated method that classifies normal and abnormal MR images and segmentation of abnormal tissues. The proposed technique consists of four stages, pre-processing of MR images, feature extraction, image classification and abnormal tissue segmentation. Initially, the images are de-noised and the features like mean, variance and wavelet components are extracted. Then the features are given to a Feed Forward Back Propagation artificial neural network for classifying the images into normal and abnormal classes. In the last stage abnormal tissues are segmented using Fuzzy C Means clustering algorithm. The results of proposed method indicate that the proposed method is superior to previous works.

Keywords: Magnetic resonance imaging, pre-processing, classification, feature extraction, neural networks, Fuzzy C Means clustering algorithm.

1. Introduction

Digital image processing is an ever expanding and vibrant area with applications reaching out into our day to day life such as medicine, space exploration, surveillance, authentication, automated industry inspection and many more [1]. Medical image processing, which is a part of digital image processing, is a dominant and constructive area for radiologists and consultants, which permits them to develop and improve their diagnosis [2]. Medical diagnostic and imaging system are all over the place in modern health care facilities [3].

Commonly, there are two fundamental kinds of medical images (1) functional images (such as SPECT or PET scans), which offer physiological information and (2) anatomical images like X-ray, CT, MRI contain minute data about heart, brain, nerves and more. MR imaging method, due to superior capability in viewing variation between soft tissues, high resolution, good contrast and non-invasive method for employing no ionization rays is extremely suitable [4].

In the associated subject, a handful of modern researches are available. Low-field Magnetic Resonance Imaging (MRI) is employed to allow real-time imaging in functioning rooms. The images produced are important for guidance and evaluation during the surgery, however very low resolution images with noise and artifacts were created because of the low signal strength.

Nur Faiza Ishak *et al* [5] have illustrated that implementation of a vibrant pre-processing algorithm to take out the brain area in low-field MRI images in order to specifically fragment the brain image. Histogram-based study states that the majority of low-field MR images contain three peaks, where the first two peaks recap the surroundings and artifacts, appropriately, while the final peak is the region-of-interest (ROI). They have offered some constructive steps that could be achieved earlier to brain fragmentation. Promising effects has been stated for both qualitative and quantitative measurements.

Dubey *et al* [6] have suggested a strategy for fragmentation process that eliminates the unfavorable effect on the boundary, which is not needed mainly from the attitude of volume delivering. Further specific boundary detection and holes filling following fragmentation was accomplished by this strategy. They have proposed a semi-automatic computation which is of volumetric size of brain tumor. A relative study of manual, more exact and improved presentation for 3D volume measurements have demonstrated by the seeded area growing and this progressive strategy. By the suggested method and improved results have been explained, two patients of different tumor type and shape have been experimented.

Image segmentation is an important and challenging issue in the medical image processing. Logeswari *et al* [7] has explained a two stage segmentation process. MRI brain image is attained from the database and the noises were separated from it after that the HSom based segmentation has been executed. HSom is the annex of Self Organizing Map that is employed at this point to classify the image row by row. An elevated volume of tumor pixels, computation speed was achieved in the lowest level by utilizing the HSom with the vector quantization.

2. Proposed Segmentation Framework

The proposed MRI brain image abnormal tissues segmentation technique segments and classifies the images based on the abnormal tissues. The proposed technique mainly comprised of four stages (i) Preprocessing (ii) Feature Extraction (iii) Image classification and (iv) Segmentation. The four stages of proposed MRI brain image abnormal tissues segmentation technique are discussed in section 2.1, 2.2, 2.3, and 2.4 respectively.

Structure of the proposed MRI brain image abnormal tissues segmentation technique is illustrated in Fig. 1.

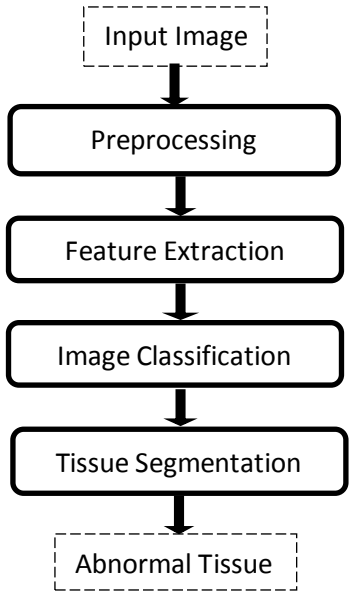

Fig. 1. Structure of the proposed MRI Brain Image Abnormal Tissues Segmentation Technique

In Fig. 1, input image from the MRI database is given to the preprocessing phase for noise removal and de-noised image is given to the feature extraction phase. In feature extraction phase, the features like mean, variance, wavelet features are extracted and given to the image classification phase. In image classification, a Feed Forward Back Propagation Neural Network (FFBNN) is used to categorize the input image into normal or abnormal. After classifying the images, the abnormal images are given to the segmentation phase for segmenting the abnormal tissues.

2.1 Preprocessing

Images usually contain one or more type of noises and artifacts. Especially in MR images, inhomogeneous magnetic field, patient motions during imaging time, thermal noise and existence of any metal things in the imaging environment are some reasons that can create noise and artifacts. So preprocessing is an important step in Medical Image Processing.

The entire MRI brain image database is divided into training and testing databases. The MRI images from both databases are given to the preprocessing phase. Before preprocessing the given images in the databases are converted into gray scale images. The gray scale images from both databases are represented as I_n' and I_m'. After the conversion the preprocessing process is performed. The different steps in the preprocessing phase are given below.

Input: Images I_n', I_m'.

Output: Noisy free image I_n'', I_m''

Step 1: Initially create a random mask P with the size of MxNx2.

$$P = \begin{bmatrix} \begin{bmatrix} (1,1) & (1,2) & \cdots & (1,N) \\ (2,1) & (2,2) & \cdots & (2,N) \\ \vdots & \vdots & \vdots & \vdots \\ (M,1) & (M,2) & \vdots & (M,N) \end{bmatrix} \\ \begin{bmatrix} (1,1) & (1,2) & \cdots & (1,N) \\ (2,1) & (2,2) & \cdots & (2,N) \\ \vdots & \vdots & \vdots & \vdots \\ (M,1) & (M,2) & \vdots & (M,N) \end{bmatrix} \end{bmatrix} \quad (1)$$

Step 2: Take the images I_n', I_m' and find the difference matrix by,

For $i = 1,2,\cdots M$

For $j = 1,2,\cdots N$

$$x(I_n^{a'}) = new(p(i+1), p(j)) = p(1,1) - (p(i+1), p(j)) \quad (2)$$

End

End

For $i = 1,2,\cdots M$

For $j = 1,2,\cdots N$

$$X(x(I_n')) = new(p(i), p(j+1))$$
$$= (p(i), p(j+1)) + p(1,1) - (p(i), p(j+1)) \quad (3)$$

End

End

The resultant matrix from the difference process is denoted as X. This same process is followed for the image $I_m^{a'}$ and gets the matrix result Y.

Step 3: Compute new matrixes X' and Y' by,

$$X' = \begin{cases} X(r(i)) = P(r(i)) ; i = 1 \\ X(r(M)) = P(r(M)) \\ X(c(j)) = P(c(j)); \ j = 1 \\ X(c(N)) = P(c(N)) \end{cases} \quad (4)$$

$$Y' = \begin{cases} Y(r(i)) = P(r(i)) ; i = 1 \\ Y(r(M)) = P(r(M)) \\ Y(c(j)) = P(c(j)); \ j = 1 \\ Y(c(N)) = P(c(N)) \end{cases} \quad (5)$$

Step 4: Update the images $I_n^{a'}, I_m^{a'}$ by,

$$I_n^{a''} = u_{I_n^{a'}}' = I_n^{a'} - \theta X' \quad (6)$$

$$I_m^{a''} = u_{I_m^{a'}}' = I_m^{a'} - \theta Y' \quad (7)$$

Step 5: Compute forward derivative by extracting the column and row values $u_{I_n^{a'}}' c(j+1), u_{I_n^{a'}}' r(i+1)$ (where j=1 to N and i=1 to M) and put into the new mask

$du^2 I_n^{a'}$ and $du^1 I_n^{a'}$. For image $u_{I_m^a}$, also we compute the forward derivative matrices $du^2 I_m^{a'}$ and $du^1 I_m^{a'}$.

$$u_{I_n^a}' = \begin{bmatrix} (1,1) & (1,2) & (1,3) & \cdots & (1,N) \\ (2,1) & (2,2) & (2,3) & \cdots & (2,N) \\ \vdots & \vdots & \vdots & \vdots & \vdots \\ (M,1) & (M,2) & (M,3) & \cdots & (M,N) \end{bmatrix} = \begin{bmatrix} 1 & 2 & 3 & N-1 & N \\ (1,2) & (1,3) & \cdots & (1,N) & (1,N) \\ (2,2) & (2,3) & \cdots & (2,N) & (2,N) \\ \vdots & \vdots & \vdots & \vdots & \vdots \\ (M,1) & (M,2) & \cdots & (M,N) & (M,N) \end{bmatrix} = du_{I_n^a}' \quad (8)$$

Step 6: Compute distinction value

$$D(I_n^{a'}) = D^1 I_n^{a'} = D^2 I_n^{a'} = (1 + ((t/\theta)/g).\times \left| \sqrt{(du^1 I_n^{a'})^2 + (du^2 I_n^{a'})^2} \right| \quad (9)$$

$$D(I_m^{a'}) = D^1 I_m^{a'} = D^2 I_m^{a'} = (1 + ((t/\theta)/g).\times \left| \sqrt{(du^1 I_m^{a'})^2} + (du^2 I_m^{a'})^2 \right| \quad (10)$$

Step 7: Modify the mask P values by,

$$P' = (P - (t/\theta).*(du^2 I_n^{a'} * du^1 I_n^{a'}).\,/\,D(I_n^{a'}) \quad (11)$$

Step 8: The process is repeated until the maximum number of iterations S is reached.

Step 9: Finally we get the noise free images $I_n^{a''}$ and $I_m^{a''}$.

Then the resultant denoised images $I_n^{a''}$ and $I_m^{a''}$ are given to the average filtering to further enhance the images for the classification process.

2.2 Feature Extraction

In feature extraction phase, five features are extracted for image classification. The extracted features are mean, variance, and multilevel 2D Haar wavelet decomposition [8] characteristics such as horizontal, vertical, diagonal bands of wavelet transform features. The procedure of feature extraction for image classification is described below.

Features are extracted from the database images I_n' and I_m' and that image pixel values are represented as P. The features like mean and variance are directly computed from the input images and the wavelet features are extracted by applying wavelet transform. In this work a two level Haar wavelet transform is applied on the input images and three features are extracted from the resulting image. The extracted five features are stated as,

$$M(I_n') = \frac{1}{M \times N} \sum_{a=1}^{M} \sum_{b=1}^{N} p_{ab} \quad (12)$$

$$E(I_n') = \left(\frac{1}{M \times N} \left(\sum_{a=1}^{M} \sum_{b=1}^{N} (p_{ab} - M(I_n'))^2 \right) \right) \quad (13)$$

$$H(I_n') = \frac{1}{c} \sum_{c=1}^{C} h_c \quad (14)$$

$$V(I_n') = \frac{1}{c} \sum_{c=1}^{C} v_c \quad (15)$$

$$D(I_n') = \frac{1}{c} \sum_{c=1}^{C} d_c \quad (16)$$

In Equ. (12), p_{mn} is the pixel value of the image and in Equ.(14), (15), and (16), h_c, v_c, d_c are the horizontal, vertical, diagonal wavelet coefficients of the image I_n'. These extracted features are given to the FFBNN for image classification process described in the following section.

2.3 Image Classification

In image classification phase, entire database images are classified into normal and abnormal classes. For the image classification, the extracted features $M(I_n')$, $E(I_n')$, $H(I_n')$, $V(I_n')$ and $D(I_n')$ are given to the FFBNN.

2.3.1 FFBNN Training and Testing

Network training and testing process is performed by using the extracted features. The basic structure of FFBNN network is shown in Fig.2. In the training phase, the MRI images are taken out from the given database. The extracted features are given to FFBNN network. The FFBNN network is well trained using these extracted features. The network is created with five input units, H_a hidden units and one output unit.

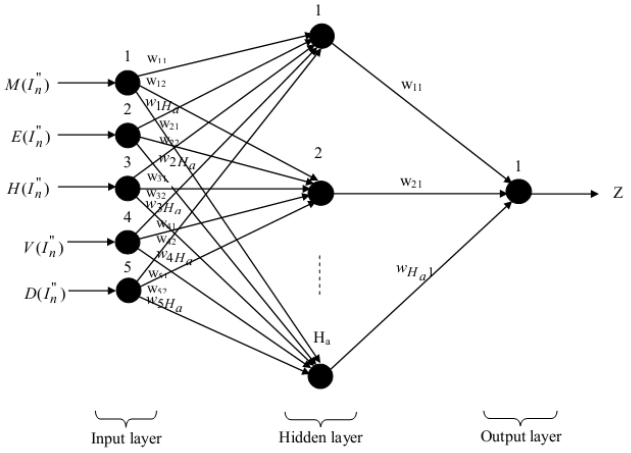

Fig.2. Basic Structure of the FFBNN

The following steps describe the function of the Neural Network:

Step 1: Initialize the weights to every neuron except the input neurons in the network.

Step 2: The neural network is designed with five neurons in the input layers, H_a hidden layers and one output layer. The weights are then added to the neural network and it is biased.
Step 3: The planned bias function and activation function for the neural network is described below.

$$B_{(I_n')} = \beta + \sum_{h=1}^{H_a} (w_{(h)} M(I_n')(h) + w_{(h)} E(I_n')(h) + w_{(h)} H(I_n')(h) + w_{(h)} V(I_n')(h) + w_{(h)} D(I_n')(h) \quad (17)$$

$$A(B_{(I_n')}) = \frac{1}{1+e^{-B(I_n')}} \quad (18)$$

The input layer bias function is given in Eq. (17). In Eq. (17) $M(I_n'), E(I_n'), H(I_n'), V(I_n')$ and $D(I_n')$, are the extracted features from the image I_n'. The activation function for the output layer is given in Eq. (18).

Step 4: Compute the learning error for the neural network.

$$L^{(e)} = \frac{1}{H_a} \sum_{h=0}^{H_a} D_h - Z_h \quad (19)$$

In Eq. (19), $L^{(e)}$ is the learning error rate of FFBNN network, D_h and Z_h are the desired and actual outputs respectively.

2.3.2 Minimization of error by back propagation algorithm

The steps involved in the training of BP algorithm based NN is given below:
(i) Weights are allocated to the hidden layer and output layer neurons by randomly chosen weights. The input layer neurons have a constant weight.
(ii) Determine the bias function by Eq. (17). The activation function is computed by Eq. (18).
(iii) Calculate BP error for each node and update the weights as follows

$$w_{(h)} = w_{(h)} + \Delta w_{(h)} \quad (20)$$

(iv) Using Eq. (20) the weight $\Delta w_{(h)}$ is changed, it can be determined as,

$$\Delta w_{(h)} = \delta . X_{(B(I_n')h)} . E^{(Bp)} \quad (21)$$

Where δ is the learning rate, which normally ranges from 0.2 to 0.5, and $E^{(Bp)}$ is the BP error.
(v) Then repeat the steps (2) and (3) until the BP error gets minimized. The process is repeated until it satisfies $E^{(Bp)} < 0.1$.
(vi)The error gets minimized to a minimum value and the FFBNN is well trained for performing the testing phase.

The result of this FFBNN network is represented as Z and this value Z is compared with threshold value t_1.

$$result = \begin{cases} Abnormal;\ Z \geq t_1 \\ Normal;\ Z < t_1 \end{cases} \quad (22)$$

In this way, the brain MRI images are classified into normal and abnormal classes.

2.4 Segmentation

In segmentation process the abnormal images $I_n^{a''}$ and $I_m^{a''}$ are segmented accurately to find the abnormal areas. The training database image abnormal tissues are manually segmented by the user. The testing database image tissues are segmented by applying Fuzzy C Means Clustering algorithm. The segmentation process in the proposed work is as follows:

2.4.1 Skull stripping

For precise fragmentation of brain abnormal tissues, skull stripping is employed. The brain cortex can be pictured as a distinct dark ring surrounding the brain tissues in the MRI images. The distinct dark ring surrounding the brain tissues are eradicated by skull stripping technique. In skull stripping, at first the given $I_m^{a''}$ images are changed into gray scale image and next a morphological operation [9] is carried out in the images. After that, by applying region based binary mask removal the brain cortex in the gray scale image is stripped. The deletion of unnecessary tissues around the images can improve the segmentation precision.

2.4.2 Abnormal Tissue Segmentation using Fuzzy C-Means Clustering Algorithm

Fuzzy C-Mean (FCM) is an unsupervised clustering algorithm that has been applied to wide range of problems involving feature analysis, clustering and classifier design. It is a data clustering technique in which a dataset is grouped into n clusters with every data point in the dataset belonging to every cluster to a certain degree. It is an approach, where the data points have their membership values with the cluster centers, which will be updated iteratively [10]. The FCM algorithm consists of the following steps:
Step 1: Let us suppose that M-dimensional N data points represented by x_i (i = 1, 2. . . N) are to be clustered.
Step 2: Assume the number of clusters to be made, that is, C, where $2 \leq C \leq N$.
Step 3: Choose an appropriate level of cluster fuzziness f > 1.
Step 4: Initialize the N × C ×M sized membership matrix U, at random, such that $U_{ijm} \in [0, 1]$ and $\sum_{j=1}^{C} Uijm = 1.0$, for each i and a fixed value of m.
Step 5: Determine the cluster centers CC_{jm}, for j^{th} cluster and its m^{th} dimension by using the expression given below:

$$CC_{jm} = \frac{\sum_{i=1}^{N} U_{ijm}^{f} x_{im}}{\sum_{i=1}^{N} U_{ijm}^{f}} \quad (23)$$

Step 6: Calculate the Euclidean distance between i^{th} data point and j^{th} cluster center with respect to, say m^{th} dimension like the following:

$D_{ijm} = ||(x_{im} - CC_{jm})||.$ (24)

Step 7: Update fuzzy membership matrix U according to D_{ijm}. If $D_{ijm} > 0$, then

$$U_{ijm} = \frac{1}{\sum_{c=1}^{C} \frac{D_{ijm}}{D_{icm}}^{\frac{2}{f-1}}}. \quad (25)$$

If $D_{ijm} = 0$, then the data point coincides with the corresponding data point of j^{th} cluster center CC_{jm} and it has the full membership value, that is, $U_{ijm} = 1.0$.

Step 8: Repeat from Step 5 to Step 7 until the changes in $U \leq \varepsilon$, where ε is a pre-specified termination criterion.
The output of segmentation algorithm is enhanced using the region properties like area, perimeter and major axis length.

3. Experimental Results and Discussion

Proposed MRI image classification and abnormal tissue segmentation technique is implemented in the working platform of MATLAB (version 7.12). The database samples, preprocessed images, classification result and segmented result are illustrated in Fig.3, Fig.4, Fig.5, and Fig.6 respectively.

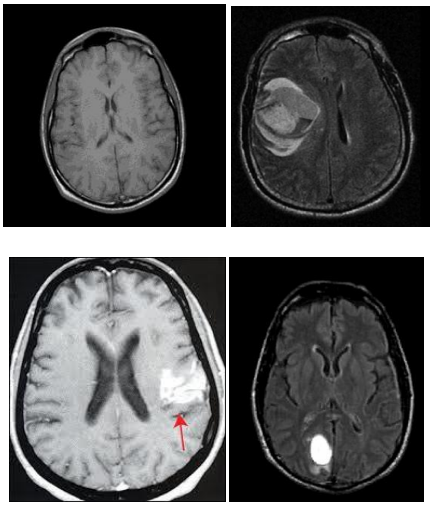

Fig. 3.Sample brain MRI normal and abnormal images

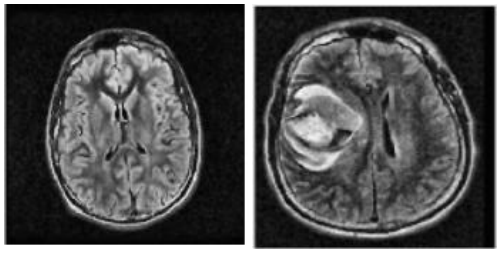

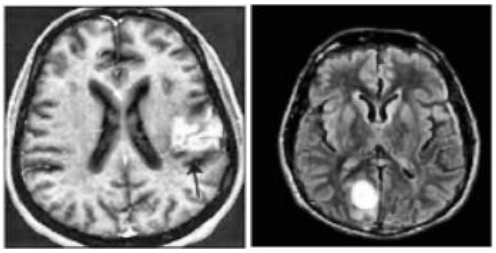

Fig. 4. Preprocessed Images

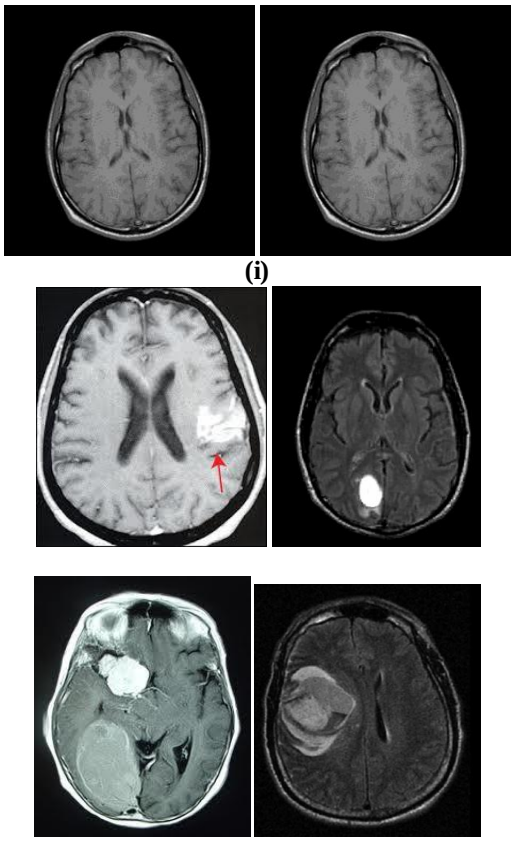

(i)

Fig. 5. Classified Image results (i) Normal (ii) Abnormal

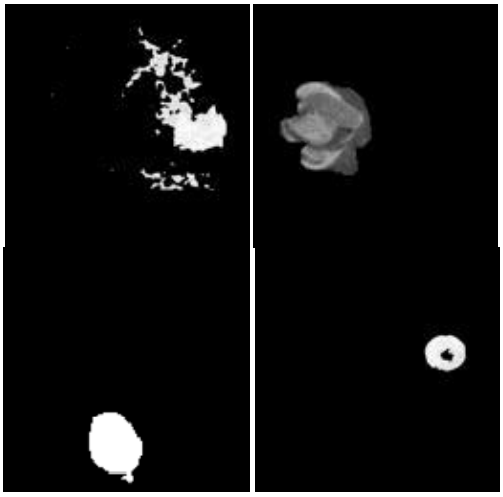

Fig.6. Segmentation result

Table1: Image Classification Result

No. of images	Correctly Classified Images	Wrongly Classified Images
42	41	1

In this work, 42 MRI brain images were considered of which 12 are normal and 30 are abnormal. By using the extracted features like, Mean, median, Variance, and wavelet features the proposed FFBNN classifies 11 images as normal and 31 as abnormal. Hence the proposed image classification process by FFBNN attained 98% classification accuracy.

3.1 Performance Analysis

In the proposed technique, classification performance is evaluated using the statistical measures like Sensitivity, Specificity and Accuracy based on the True Positive (TP), False Positive (FP), True Negative (TN) and False Negative (FN) values. Fig.7 illustrates the performance evaluation of image classification phase.

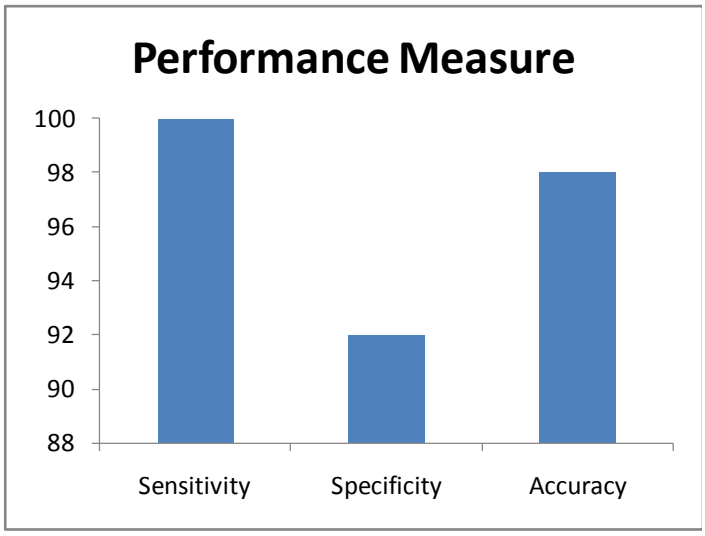

Fig.7 Performance evaluation of image classification

In the proposed technique, segmentation performance is evaluated by two evaluation metrics namely, Tanimoto Coefficient (TC), and Dice Coefficient (DC). Moreover the classification performance result by the FFBNN technique is analyzed by the statistical measures which are given in [11]. The evaluation metrics are computed in the segmentation process are determined by the following Equations,

(i) Dice Coefficient (DC):

$$DC = \frac{2|R_o \cap R_a|}{|R_o| + |R_a|} \tag{36}$$

(ii) Tanimoto Coefficient (TC)

$$TC = \frac{|R_o \cap R_a|}{|R_o \cup R_a| - |R_o \cap R_a|} \tag{37}$$

The evaluation metrics DC and TC is computed by defining the ratio between intersection and union of two sets R_o and R_a, representing the obtained and actual segmentations, respectively. The segmentation performance evaluation metrics results calculated for some of the images are given in Table II.

Table 2: Performance of Proposed Technique Segmentation process in terms of evaluation Metrics DC andTCTC

Images	R_o	R_a	DC	TC
Image-1	6053	11759	0.57916	0.407618
Image-2	20080	8481	0.369385	0.226531
Image-3	63	63	1	1
Image-4	63	63	1	1
Image-5	3790	3307	0.647598	0.47885
Image-6	5453	8573	0.669756	0.503484
Image-7	2949	2210	0.62454	0.454059
Image-8	3457	3457	1	1
Image-9	947	1674	0.645555	0.47662
Image-10	4558	2934	0.555526	0.384587

4. Conclusion

This paper proposes an efficient MRI abnormal tissues segmentation technique which effectively segments MRI abnormal tissues. Initially, noises in the MRI images were removed and classified based on the extracted features. Afterward, the classified abnormal images tissues were segmented. The performance of the proposed technique is evaluated by more number of MRI images. The implementation result shows that the proposed MRI abnormality tissues segmentation technique efficiently segments and classifies the MRI abnormal images based on the abnormal tissues than the existing classifier. Experimental results show that the proposed technique is more effective in segmenting abnormal tissues and high classification accuracy than the existing classifier.

References

[1] Daggu Venkateshwar Rao, Shruti Patil, Naveen Anne Babu and Muthukumar, "Implementation and Evaluation of Image Processing Algorithms on Reconfigurable Architecture using C-based Hardware Descriptive Languages", International Journal of Theoretical and Applied Computer Sciences, Vol. 1, No. 1, pp. 9-34, 2006.

[2] Ghrare, Mohd. Ali, Jumari and Ismail, "An Efficient Low Complexity Lossless Coding Algorithm for Medical Images", American Journal of Applied Sciences, Vol. 6, No. 8, pp. 1502-1508, 2009.

[3] Brintha Therese and Sundaravadivelu, "Bipolar Incoherent Image Processing for Edge Detection of Medical Images", International Journal of Recent Trends in Engineering, Vol. 2, No. 2, pp. 229-232, November 2009.

[4] AmirEhsan and Lashkari, "A Neural Network based Method for Brain Abnormality Detection in MR Images Using Gabor Wavelets", *International Journal of Computer Applications*, Vol. 4, No.7, pp. 9-15, July 2010.

[5] Nur Faiza Ishak, Rajasvaran Logeswaran and Wooi-Haw Tan, "Artifact and noise stripping on low-field brain MRI", *International Journal of Biology and Biomedical Engineering*, Vol. 2, No. 2, pp. 59-68, 2008.

[6] Dubey, Hanmandlu, Gupta and S. K. Gupta, "An Advanced Technique for Volumetric Analysis", International Journal of Computer Applications, Vol. 1, No. 1, pp. 91-98, February 2010.

[7] Logeswari and Karnan, "An improved implementation of brain tumor detection using segmentation based on soft computing", *Journal of Cancer Research and Experimental Oncology*, Vol. 2, No. 1, pp. 6-14, March 2010.

[8] Radomir S. Stankovic and Bogdan J. Falkowski, "The Haar wavelet transform: its status and achievements", *Computers and Electrical Engineering*, Vol. 29, pp. 25–44, 2003.

[9] Soumya Maitra, "Morphological Edge Detection Using Bit-Plane Decomposition in Gray Scale Images", In Proceedings of INDIA Com, New Delhi, 2011.

[10] P Vasuda and S Satheesh, "Improved Fuzzy C-Means Algorithm for MR Brain Image Segmentation", International Journal on Computer Science and Engineering, Vol. 02, No. 05, 2010, pp. 1713-1715.

[11] http://en.wikipedia.org/wiki/Sensitivity_and_specificity.